Appl Phys B (2012) 109:407–414
DOI 10.1007/s00340-012-5005-x

Applied Physics B
Lasers and Optics

Linewidth of a quantum-cascade laser assessed from its frequency noise spectrum and impact of the current driver

L. Tombez · S. Schilt · J. Di Francesco · T. Führer · B. Rein · T. Walther · G. Di Domenico · D. Hofstetter · P. Thomann

Received: 23 November 2011 / Revised version: 24 February 2012 / Published online: 21 April 2012

Abstract We report on the measurement of the frequency noise properties of a 4.6-μm distributed-feedback quantum-cascade laser (QCL) operating in continuous wave near room temperature using a spectroscopic set-up. The flank of the R(14) ro-vibrational absorption line of carbon monoxide at 2196.6 cm^{-1} is used to convert the frequency fluctuations of the laser into intensity fluctuations that are spectrally analyzed. We evaluate the influence of the laser driver on the observed QCL frequency noise and show how only a low-noise driver with a current noise density below ≈1 nA/$\sqrt{}$Hz allows observing the frequency noise of the laser itself, without any degradation induced by the current source. We also show how the laser FWHM linewidth, extracted from the frequency noise spectrum using a simple formula, can be drastically broadened at a rate of ≈1.6 MHz/(nA/$\sqrt{}$Hz) for higher current noise densities of the driver. The current noise of commercial QCL drivers can reach several nA/$\sqrt{}$Hz, leading to a broadening of the linewidth of our QCL of up to several megahertz. To remedy this limitation, we present a low-noise QCL driver with only 350 pA/$\sqrt{}$Hz current noise, which is suitable to observe the ≈550 kHz linewidth of our QCL.

L. Tombez (✉) · S. Schilt · J. Di Francesco · G. Di Domenico · D. Hofstetter · P. Thomann
Laboratoire Temps-Fréquence, Institut de Physique, Université de Neuchâtel, Avenue de Bellevaux 51, 2000 Neuchâtel, Switzerland
e-mail: lionel.tombez@unine.ch
Fax: +41-21-7182511

T. Führer · B. Rein · T. Walther
Institut für Angewandte Physik, AG Laser und Quantenoptik, Technische Universität Darmstadt, Schlossgartenstr. 7, 64289 Darmstadt, Germany

1 Introduction

Since their first demonstration in 1994 [1], quantum-cascade lasers (QCLs) have been widely deployed in many types of application, especially in high-resolution spectroscopy and trace gas sensing. In trace gas sensing, QCLs have been implemented with the most widespread spectroscopic techniques, including long-path length [2], balanced detection [3], wavelength modulation spectroscopy [4], frequency modulation spectroscopy [5], photoacoustic or quartz-enhanced photoacoustic spectroscopy [6, 7] and cavity ring-down spectroscopy [8]. The characteristics of QCLs have continuously been improved in the past decade, e.g. in terms of output power, wavelength coverage or temperature of operation. One of the most essential properties for high-resolution spectroscopy is the laser spectral purity. Distributed-feedback (DFB) gratings have been implemented to make single mode, continuously tunable QCLs [9]. The first DFB-QCLs were operating in pulsed mode and consequently suffered from an important chirp resulting from the thermal heating of the laser structure during the current pulses. Even with pulses as short as 5 ns, the effective linewidth of pulsed QCLs was in the range of 250 MHz [10], while longer pulses (10–50 ns) led to a linewidth larger than 1 GHz [11, 12]. The achievement of continuous-wave (cw) DFB-QCLs [13] was a major step towards the application of the QCL technology in high-resolution spectroscopy. For example, a linewidth at the megahertz level was determined for a 4.3-μm DFB-QCL from the width of a Lamb-dip obtained in a saturation spectroscopy experiment [14].

As a result of their small linewidth enhancement factor [15] and the presence of ultrafast non-radiative processes [16], QCLs have a narrow intrinsic (or "instantaneous") linewidth [17]. However, they are subject to

flicker noise like any semiconductor device. Therefore, their linewidth strongly broadens compared to the Schawlow–Townes limit [18] at any observable timescale. Recently, Bartalini and co-workers measured the frequency noise power spectral density (PSD) of a 4.3-μm cw DFB-QCL operated at cryogenic temperature [19]. Because of the presence of flicker noise, the measured frequency noise spectrum corresponds to a linewidth in the range of several megahertz. More recently, we reported a frequency noise PSD 100 times lower for a similar DFB-QCL at a close wavelength of 4.6 μm, but operated at room temperature [20]. This corresponds to a sub-MHz linewidth at any observation times of up to 1 s. To achieve such a narrow free-running linewidth, one has to take care of the laser driver, in such a way that the current noise does not degrade the laser frequency noise and, therefore, broadens the linewidth. In this paper, we used a spectroscopic set-up to measure the frequency noise of a QCL. We discuss the impact of the driver current noise to the laser frequency noise by comparing experimental results obtained with two different drivers. From the measured frequency noise spectra, we assess the impact of these drivers to the laser linewidth. One of the drivers used in our experiments is a low-noise current source developed at TU Darmstadt. The current noise of this driver is small enough to allow the frequency noise inherent[1] to the laser to be observed, without degradation induced by the driver. In a second part, we discuss how a driver with a larger current noise impacts the linewidth of a QCL.

2 Theoretical background: relation between laser frequency noise and linewidth

The spectral properties of a laser are commonly described by its linewidth, i.e. the full width at half maximum (FWHM) of the optical lineshape. The linewidth of a laser can be experimentally determined from the heterodyne beat with a reference laser source or by self-homodyne/heterodyne interferometry using a long optical delay line [21]. The linewidth is a single parameter widely used to characterize the laser spectral properties, as it allows for a simple and straightforward comparison between different laser sources. However, this specific parameter gives an incomplete picture of the actual frequency noise of the laser. In particular, it does not contain any information about the spectral distribution of the noise. This is in contrast to the PSD of the laser frequency fluctuations, which gives a complete picture of the laser frequency noise, showing how the different noise spectral components contribute to the laser linewidth. The measurement of the frequency noise of a laser requires an optical frequency discriminator to convert the laser frequency fluctuations into intensity fluctuations that can be measured with a photodiode. An optical frequency discriminator is a device that displays a frequency-dependent transmission in a restricted frequency range, such as a gas-filled cell near an atomic/molecular resonance (Doppler-broadened [19, 20, 22] or sub-Doppler [23]), a Fabry–Pérot resonator [24] or an unbalanced two-beam interferometer [25].

From the frequency noise PSD, the laser lineshape and, thus, the linewidth, may be retrieved, but the reverse process (i.e. determining the exact frequency noise spectrum from the lineshape) is not possible. However, the exact determination of the linewidth from the frequency noise spectral density is not straightforward in most cases. This problem has been theoretically addressed for a long time [26–29] and involves a two-step integration procedure as detailed in [30]. The first step consists of calculating the autocorrelation function of the electrical field $\Gamma_{\mathrm{E}}(\tau)$ as an exponential of the integral of the frequency noise PSD filtered by a sinc^2 function [26]. Then, the optical spectrum $S_{\mathrm{E}}(\nu)$ is obtained in the second step by Fourier transform of $\Gamma_{\mathrm{E}}(\tau)$. However, only the ideal case of a pure white frequency noise can be analytically solved [27], leading to the well-known Lorentzian lineshape described by the Schawlow–Townes–Henry linewidth [15, 18]. In all other cases, including real laser frequency noise spectra encountered in practice, the procedure is far from straightforward and must be performed by numerical integration. We recently proposed a very simple approximation to determine the linewidth of a laser from an arbitrary frequency noise spectrum [30]. We showed how the frequency noise PSD spectrum $S_{\delta\nu}(f)$ can be geometrically separated into two areas (the slow and fast modulation areas) by a single line displayed in Fig. 1 that we refer to as the β-separation line, defined as $S_{\delta\nu}(f) = (8\ln(2)/\pi^2)\cdot f$. Frequency noise in these two areas has a completely different impact on the laser lineshape. Only the slow-modulation area, for which $S_{\delta\nu}(f) > (8\ln(2)/\pi^2)\cdot f$, contributes to the linewidth of the signal. The fast modulation area ($S_{\delta\nu}(f) < (8\ln(2)/\pi^2)\cdot f$) only affects the wings of the lineshape, without contributing to the linewidth. As a result, the linewidth can be approximated with a good accuracy (better than 10 %) from the surface A of the slow-modulation area,

$$\mathrm{FWHM} = \sqrt{8\ln(2)A}. \tag{1}$$

The surface A corresponds to the geometrical area under the frequency noise PSD obtained for all Fourier frequencies

[1] In this paper, we introduce the notion of frequency noise *inherent* to the laser, not to be confused with the commonly used concept of *intrinsic* frequency noise of the laser. The intrinsic frequency noise represents the white frequency noise induced by spontaneous emission in the laser and is related to the intrinsic linewidth described by the Schawlow–Townes relation [18]. Here, the frequency noise inherent to the laser corresponds to the frequency noise originating from the laser itself, without any contribution from the current source. It includes the contributions of both the flicker noise and the intrinsic noise of the laser.

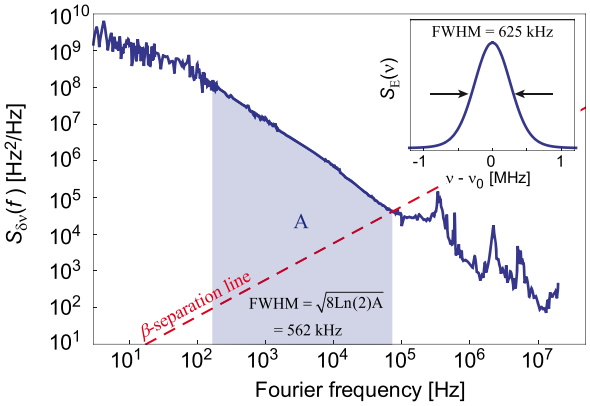

Fig. 1 Typical frequency noise spectrum of a QCL, composed of flicker $(1/f)$ noise. The laser linewidth can be approximated from the surface A (colored area in the plot) of the slow-modulation area for which the frequency noise PSD exceeds the β-separation line $(S_{\delta\nu}(f) > (8\ln(2)/\pi^2) \cdot f)$. *Inset*: lineshape calculated from the exact 2-step integration of the frequency noise spectrum [26, 30] and corresponding FWHM linewidth. In both cases a low-frequency cutoff of 200 Hz is introduced, corresponding to 5 ms of observation time

for which $S_{\delta\nu}(f)$ exceeds the β-separation line. In the case of a typical frequency noise spectrum dominated by flicker $(1/f)$ noise, as illustrated in Fig. 1 for our QCL, the surface A diverges at low frequency. Therefore, a low-frequency cutoff f_c has to be introduced, which represents the inverse of the observation time τ_o in which the linewidth is measured ($f_c = 1/\tau_o$). In such a case, the surface A is bounded by f_c at low frequency and by the crossing point with the β-separation line at high frequency (as the noise at higher frequency is lower than the β-separation line and thus does not contribute to the linewidth. The principle of our linewidth approximation is shown in Fig. 1 in the case of a real frequency noise spectrum (corresponding to our QCL). The approximated linewidth calculated from Eq. (1) is 562 kHz if we consider a low cutoff frequency $f_c = 200$ Hz (corresponding to an observation time τ_o of 5 ms). This is in good agreement with the linewidth of 625 kHz extracted from the lineshape function computed from the exact 2-step numerical integration of the frequency noise spectrum, shown in the inset of Fig. 1.

3 Measurement set-up

3.1 Quantum-cascade laser

The laser used in the experiment is a 4.6-μm DFB-QCL from Alpes Lasers SA, Switzerland, with continuous-wave single-mode operation at room temperature. The laser is temperature-stabilized at 278 K with a one-stage thermoelectrical cooler. At this temperature, the threshold current is 290 mA. The laser is usually operated at 350 mA to be tuned to a molecular absorption line for the frequency noise measurements (see Sect. 3.3 for more details). Under these conditions, the laser output power is ≈6 mW and the bias voltage is 10 V.

3.2 Laser drivers

The QCL was driven with two different current sources to assess the impact of the current noise of the driver on the laser frequency noise and linewidth. The first driver, labeled Driver-1, is a home-made current source initially developed to drive standard laser diodes. It was modified to support the higher operating voltage of QCLs and can deliver a current in the range of 0–500 mA at a bias voltage of up to 12 V at the maximum current value. The current noise of this driver, measured on a resistive load (30 Ω) at the same voltage and current as used to drive the QCL, is around 2 nA/$\sqrt{}$Hz. This value is not good enough not to affect the measured frequency noise of our QCL, and therefore a better source was developed.

The second driver, labeled Driver-2, is a QCL current source developed at TU Darmstadt. It is based on the original design of Libbrecht and Hall [31]. However, some modifications listed below are implemented in order to meet the specific requirements of the QCLs regarding compliance voltage and operating current. It also features the option of an additional modulation input which can be used, e.g., for various locking schemes.

To achieve a current of 500 mA at 12 V, the supply voltage has been increased to ±18 V, which is the specified maximum voltage for the operational amplifiers. Furthermore, the value of the current sense resistor has been decreased to 10 Ω, representing the maximum value taking into account the dropout of the voltage regulator (LM317). For the MOSFET and the coil, components with a low resistive load have been selected to ensure a low power dissipation. Consequently, no active air cooling is required. Since QCLs are quite sensitive devices, all supply voltages are switched using solid-state relays, which show no bouncing and/or potential voltage spikes. Furthermore, the relays are controlled such that the supply voltages for the controller integrated circuits are switched on before the power supply voltage for the QCL itself and vice versa during the power off sequence, thus preventing damage to the QCL. The current driver features two external modulation input. A fast modulation of up to 15 MHz is suited for fast frequency modulation of the laser via its drive current, e.g. for Pound–Drever–Hall locking [32]. In this case, the modulation amplitude is up to 10 mA. In addition, a slow-modulation input allows a full scale current modulation at lower frequencies of up to 100 kHz. This modulation input can be used to feed back a correction signal to control the laser frequency in a stabilization loop.

To minimize the noise figure of the driver, care has been taken regarding its implementation. A four-layer board with

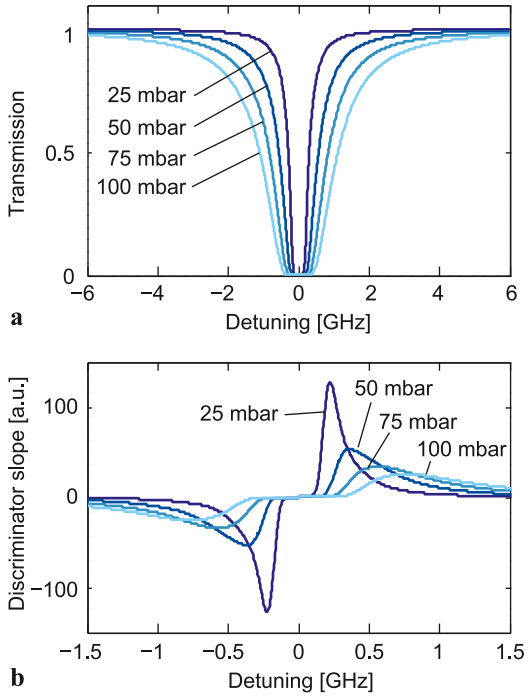

Fig. 2 (**a**) Simulated transmission for the R(14) absorption line of CO at 2196.6 cm^{-1} through a 1-cm long cell filled with pure CO at different pressures (25, 50, 75 and 100 mbar). (**b**) Corresponding frequency-to-amplitude conversion factor as a function of the laser detuning from the line center, determined as the derivative of the transmission curves (**a**)

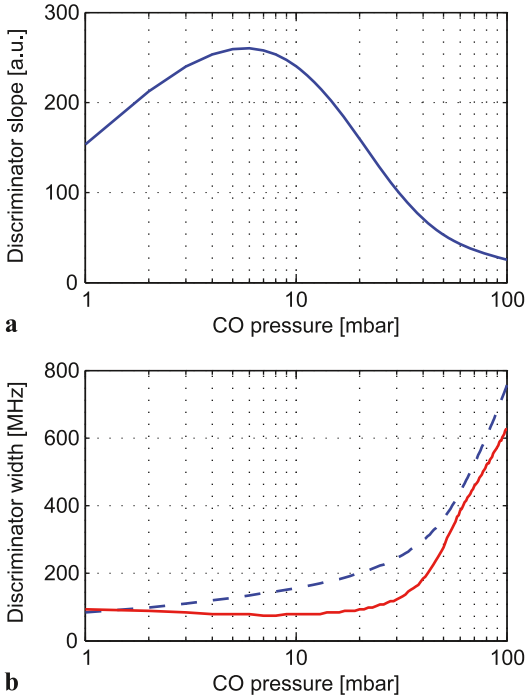

Fig. 3 (**a**) Variation of the calculated discriminator slope corresponding to the R(14) absorption line of CO as a function of the gas pressure. A 1-cm long gas cell filled with pure CO is considered. (**b**) Spectral width of the CO frequency discriminator (*red plain curve*) as a function of the CO pressure. The discriminator width is defined as the laser tuning range in which the CO frequency-to-amplitude conversion factor is within 10 % of the value shown in (**a**). The *dashed* (*blue*) *curve* represents the detuning from the line center at which the maximum discriminator slope occurs

separate ground-, signal- and supply-layers has been manually routed while paying particular attention to short routes at the critical points as well as proper grounding and shielding. Furthermore, only ultra-low-noise operational amplifiers in SMD (Surface Mount Device) packages were employed. Noise measurements reveal a maximum current noise density of 1.5 nA/$\sqrt{}$Hz with the slow-modulation feature enabled and 350 pA/$\sqrt{}$Hz without slow-modulation, respectively, measured on a resistive load in the same conditions as for Driver-1.

3.3 Optical frequency discriminator

We use the flank of a molecular absorption line as an optical frequency discriminator as previously employed in [19, 20, 22]. Carbon monoxide (CO) is used in our set-up as a result of the good spectral overlap between the QCL emission wavelength and the fundamental ($0 \rightarrow 1$) vibrational band of CO. With a proper adjustment of the laser temperature (coarse tuning) and current (fine tuning), the laser wavelength coincides with the R(14) ro-vibrational transition of CO at 2196.6 cm^{-1}. Owing to the strong absorption of the CO fundamental vibrational band (the linestrength of the R(14) line is 2.01×10^{-19} $cm^{-1}/(molecule \cdot cm^{-2})$), a single pass absorption cell with a pathlength as short as 1 cm is sufficient to produce a large absorption. Figure 2a shows a simulation of the transmission through a 1-cm long cell at different CO pressures. Spectroscopic parameters from HITRAN08 database [33] have been used to compute the CO Voigt lineshape. For faster computation, the analytical approximation of the Voigt profile given by Whiting [34, 35] has been used. From the computed transmission curves, the frequency-to-amplitude conversion factor, which is referred to as the discriminator slope D_ν, has been determined as a function of the laser detuning (Fig. 2b). The maximum discriminator slope is achieved in the steepest part of the CO transmission curve. Figure 3a shows how the cell filling can be optimized to maximize the discriminator slope. The optimal CO pressure is 6 mbar for a 1-cm long cell.

A scheme of our experimental set-up is shown in Fig. 4. The laser beam is collimated with an aspheric ZnSe lens and propagates through a 1-cm long gas cell filled with pure CO. The CO cell pressure was generally 20 mbar in our experiments. This is larger than the optimal pressure of 6 mbar determined from Fig. 3a, but the corresponding 40 % reduction of the CO discriminator slope is not so important. Indeed, the flank of the CO line remains steep enough to properly convert the laser frequency noise into intensity noise

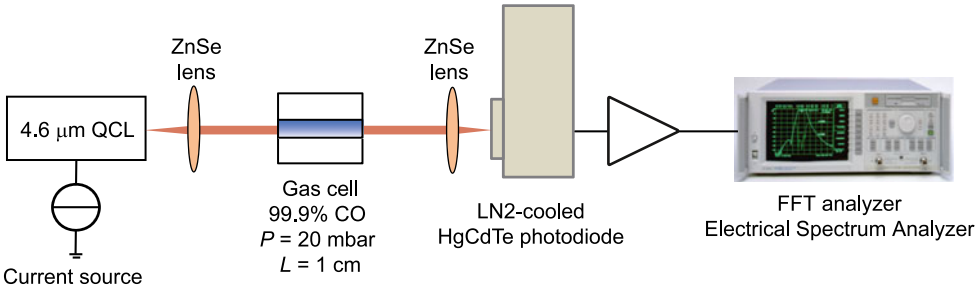

Fig. 4 Scheme of the experimental set-up used for the measurement of the QCL frequency noise

even at high Fourier frequencies. The laser is tuned to the flank of the CO absorption profile, where the frequency-dependent transmission linearly converts the frequency fluctuations of the laser into intensity variations. Behind the cell, another ZnSe lens focuses the transmitted light onto a low-noise liquid-nitrogen-cooled HgCdTe detector with 20-MHz bandwidth. The amplitude fluctuations of the detector signal are measured with a fast Fourier transform (FFT) analyzer (Stanford Research System SRS770) for low Fourier frequencies (up to 100 kHz) and with an electrical spectrum analyzer (ESA), model Agilent E4407B, at higher frequencies. To achieve a good spectral resolution over the entire considered frequency range, each measured spectrum is obtained from the combination of five FFT spectra of decreasing spectral resolution (span of 0.024, 0.195, 1.56, 12.5 and 100 kHz) and of three ESA spectra (span 200–800 kHz, 1.6–6.4 MHz and 12.8–51.2 MHz). Each of these spectra is obtained by co-averaging 200 individual FFT traces or 50 ESA traces. The PSD of the detector output voltage is transformed into frequency noise PSD of the laser by normalization with the squared value of the measured discriminator slope D_ν ($D_\nu = 23$ mV/MHz). This scaling factor is determined from the recorded cell transmission obtained by scanning the laser through the CO line. A linear fit of the flank of the CO transmission profile provides the discriminator slope.

4 Experimental results

We measured the frequency noise spectrum of our QCL driven by the two current sources described in Sect. 3.2 using the optical frequency discriminator detailed in Sect. 3.1. Results are shown in Fig. 5. The contribution of the laser intensity noise to the measured spectra is also shown to demonstrate that the observed noise actually corresponds to laser frequency fluctuations converted into amplitude noise by the CO-line frequency discriminator, and does not directly result from laser intensity fluctuations. The laser intensity noise was measured using the same set-up, with the laser detuned from the CO transition and using the same average optical power impinging on the photodetector as for the frequency noise measurements. The contribution of

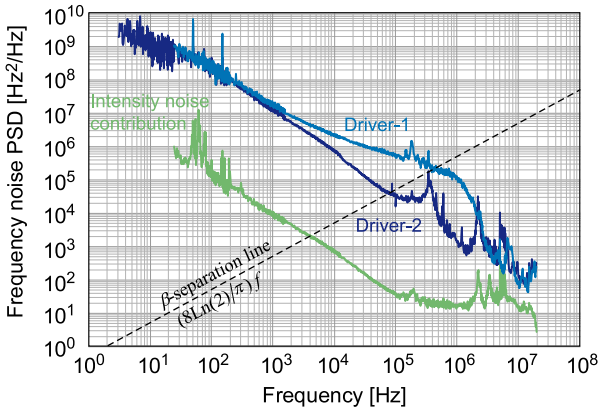

Fig. 5 Frequency noise of a 4.6-μm DFB-QCL operated at 278 K measured with the use of two current drivers with a different current noise (Driver-1: ≈2 nA/$\sqrt{}$Hz; Driver-2: ≈350 pA/$\sqrt{}$Hz). The frequency noise of the laser is almost unaffected when Driver-2 is used, whereas the current noise contribution becomes significant and creates excess frequency noise between 1 kHz and 3 MHz when Driver-1 is used

the laser intensity noise to the measured frequency noise PSD (see Fig. 5) was obtained by scaling the PSD of the photodetector output voltage by $1/D_\nu^2$. Finally, the contribution of the photodetector and amplifier, measured with the laser beam blocked and scaled into an equivalent frequency noise in the same way, was determined to be negligible (<10 Hz^2/Hz),

It is clearly apparent from Fig. 5 that excess frequency noise is observed in the range from 1 kHz to 3 MHz with the use of Driver-1. On the other hand, we verified that the noise spectrum measured with the use of Driver-2 corresponds to the frequency noise inherent to the laser, without any deterioration induced by the driver noise [20], apart for the small bumps visible around 400 kHz and at higher frequencies. The laser frequency noise shows a continuous $1/f^\alpha$ behavior for all Fourier frequencies with α close to 1. The behavior in the high frequency region ($f > 100$ kHz) is hidden by spurious noise peaks induced by the current source but the general $1/f$ trend remains visible. Therefore, there is no clear indication in our data that the laser white frequency noise is reached at Fourier frequencies up to 10 MHz. This is in contrast to interband semiconductor lasers, for which a $1/f$ corner is commonly observed near 100 kHz. Although

the white frequency noise level is not clearly observed in our spectra, the $1/f$ corner observed in other works [19] indicates that we should not be far from it. As a consequence, an upper limit $S_w \leq 100$ Hz^2/Hz can be assessed for the white frequency noise, corresponding to an intrinsic linewidth[2] $\Delta\nu_{int} = \pi \cdot S_w \leq 320$ Hz.

The excess frequency noise observed with Driver-1 occurs in the spectral range where the contribution of the current source becomes comparable to the frequency noise inherent to the laser. On the low-frequency side, this is the case when the frequency noise inherent to the laser drops below 10^7 Hz^2/Hz, corresponding to the white frequency noise contribution of the driver (white current noise of 2 nA/$\sqrt{}$Hz combined with the laser tuning coefficient of 900 MHz/mA [20]). At higher frequencies, the current fluctuations have much less effect on the laser frequency because of the ≈100 kHz bandwidth of the laser tuning response (laser frequency transfer function) [20]. As a result, the frequency noise spectra obtained with the two drivers overlap at Fourier frequencies above ≈3 MHz, where the drivers contribution becomes negligible compared to the frequency noise inherent to the laser. Therefore, there is a spectral range where the laser spectral properties are deteriorated by the noise of the current driver. The boundaries of this spectral range depend mainly on the current noise of the driver as well as on the magnitude and cutoff frequency of the QCL tuning response.

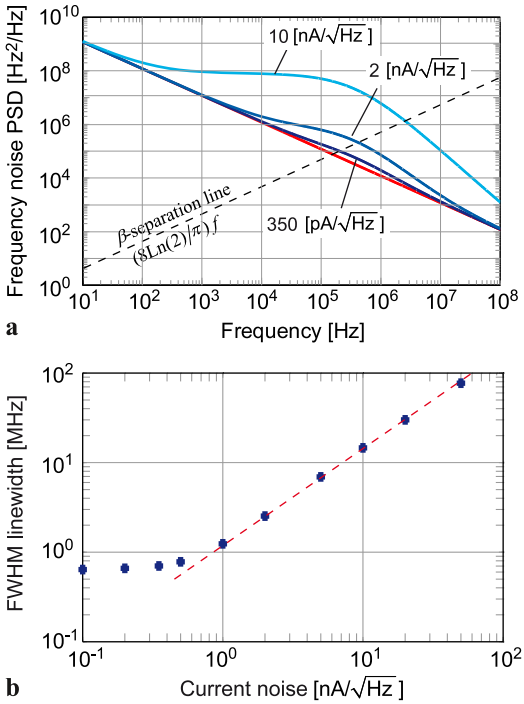

Fig. 6 (**a**) Simulation of the laser frequency noise corresponding to drivers with different current noise densities. The *lowest* (*red*) *curve* represents the modeled frequency noise inherent to the laser. (**b**) Calculated laser linewidth (FWHM) as a function of the driver current noise density (white current noise is considered). While the impact of the current driver is moderate up to 2 nA/$\sqrt{}$Hz, the linewidth reaches 20 MHz for 10 nA/$\sqrt{}$Hz of current noise. The *dashed curve* represents the linear broadening rate (≈1.6 MHz/(nA/$\sqrt{}$Hz)) of the laser linewidth as a function of the current noise

The increase of the QCL frequency noise due to the current source leads to a broadening of the laser linewidth, calculated from Eq. (1). In the present case, the laser linewidth broadens from ≈550 kHz (Driver-2) to almost 1.5 MHz (Driver-1) for an observation time of 5 ms and increases slowly for longer observation times. While the linewidth broadening is rather moderate in that case, it can become dramatic for laser drivers with a higher current noise. Based on the formalism of Sect. 2, we simulated the impact of different current noise levels to the linewidth of our laser. We considered a modeled $1/f$ laser noise PSD with a value of 10^7 Hz^2/Hz at 1 kHz, to which the contribution of different current noise levels was added. The measured tuning response of our laser (tuning coefficient of 900 MHz/mA with a cutoff frequency of 100 kHz [20]) was used to convert the driver current noise into laser frequency noise. White current noise was considered for each driver, since it is the most representative noise of typical laser drivers in the frequency range relevant for this study. Results are shown in Fig. 6a for three different noise levels of 350 pA/$\sqrt{}$Hz, 2 nA/$\sqrt{}$Hz and 10 nA/$\sqrt{}$Hz. The two first values approximate very well the noise of the two laser drivers used in our experiments and the computed frequency noise spectra

[2] A further interesting point when discussing the frequency noise of a laser is the white noise component S_w, which is directly related to the laser intrinsic linewidth by $\Delta\nu_{int} = \pi \cdot S_w$ [24, 26, 29]. The intrinsic linewidth corresponds to the Schawlow–Tones linewidth given by [15, 18]:

$$\Delta\nu_{ST} = \frac{v_g^2 h\nu n_{sp}\alpha_{tot}\alpha_m(1+\alpha_e^2)}{4\pi P_0}.$$

As mentioned in Sect. 1, the linewidth enhancement factor α_e is close to 0 in QCLs and notably lower than in other semiconductor lasers (typical value in the range 2–10 [36]). Theoretical considerations about the intrinsic linewidth in QCLs have also led to the modified Schawlow–Townes formula introduced by Yamanishi and co-workers [16]. The Schawlow–Townes linewidth can be computed from the above expression where both the total losses α_{tot} (mirror and waveguide) and the mirror losses α_m must be known. While the total losses can be straightforwardly determined in a Fabry–Pérot laser, this is not the case in a DFB laser as the losses of the grating (α_{DFB}) have to be accounted for. To estimate the total losses in our DFB, we compared its threshold current with those of a similar Fabry–Pérot device. Assuming similar waveguide losses $\alpha_{wg} = 4.5$ cm^{-1} in both cases (measured by the manufacturer on Fabry–Pérot devices) and using typical values of the laser parameters provided by the manufacturer, the losses of the grating are estimated to $\alpha_{DFB} = 1.47$ cm^{-1}. The estimated losses are in good agreement with literature data [37] for a 9-µm QCL ($\alpha_{wg} = 6.7$ cm^{-1}, $\alpha_{DFB} = 0.7$ cm^{-1}). With the spontaneous emission coefficient $n_{sp} = 1$, optical power $P_0 = 6$ mW and $\alpha_e = 0$, we calculate an intrinsic linewidth $\Delta\nu_{ST} \approx 380$ Hz, which is close to the upper limit of the white frequency noise experimentally assessed from Fig. 5.

are in good qualitative agreement with the measured spectra. The highest current noise of 10 nA/$\sqrt{}$Hz typically corresponds to some commercial QCL drivers and illustrates how the use of such drivers can increase the frequency noise of a QCL. From the computed frequency noise spectra, the corresponding linewidths were calculated as a function of the current noise using Eq. (1). Results are shown in Fig. 6b for an observation time of 10 ms. While the linewidth is almost not affected for current noise densities $\leq$ 1 nA/$\sqrt{}$Hz (corresponding to Driver-2) and only moderately with 2 nA/$\sqrt{}$Hz (Driver-1), it is drastically broadened for larger current noise, at a rate of $\approx$1.6 MHz/(nA/$\sqrt{}$Hz). As an example, the calculated linewidth reaches 20 MHz for a current noise density of 10 nA/$\sqrt{}$Hz. This linewidth broadening arises from both the resulting higher laser frequency noise PSD and the larger frequency range contributing to the laser linewidth (given by the crossing point of the noise spectrum with the β-separation line). This result illustrates how a noisy laser driver can deteriorate the linewidth of a QCL and shows that a great care must be taken in the selection of a proper current source when narrow-linewidth operation is required. However, it is important to note that the lower the frequency noise inherent to the laser, the more important becomes the contribution of the current driver. In that sense, the impact of the laser driver is more critical in the present case of our room-temperature QCL than for cryogenic QCLs, which showed to be much noisier than room-temperature devices [19, 20, 38]. Therefore, the requirements on the driver noise are much less stringent for a cryogenic QCL since the inherent linewidth is broader, typically at the level of several megahertz [19].

5 Discussion and conclusion

We described a spectroscopic experiment aiming at characterizing the frequency noise of a DFB-QCL at 4.6 µm. The R(14) ro-vibrational absorption line of CO in the fundamental ($0 \rightarrow 1$) band at 2196.6 cm^{-1} was used as a frequency discriminator to convert the frequency fluctuations of the QCL into intensity fluctuations, subsequently detected with a fast photodiode. With this set-up, we investigated the impact of the current noise of the laser driver on the QCL frequency noise. Only a carefully designed low-noise laser driver with a typical current noise of 350 pA/$\sqrt{}$Hz enabled us to observe the inherent frequency noise of the laser up to Fourier frequencies $f > 100$ kHz. The laser frequency noise essentially consists of $1/f^{\alpha}$ noise with a value of 10^7 Hz^2/Hz at $f = 1$ kHz and decreasing down to $\approx$100 Hz^2/Hz at $f = 10$ MHz. We experimentally showed how the use of a driver with a marginally larger noise (2 nA/$\sqrt{}$Hz) slightly degrades the laser spectral properties, broadening the QCL linewidth from $\approx$550 kHz to $\approx$1.5 MHz (at 10 ms observation time), as calculated from the frequency noise PSD using a simple formula. Then, we showed how the QCL linewidth would be even more dramatically broadened when the noise of the driver increases. In the case of a pure $1/f$ laser noise with 10^7 Hz^2/Hz at $f = 1$ kHz, similar to our QCL, we determined a linewidth broadening rate of 1.6 MHz/(nA/$\sqrt{}$Hz) as a function of the current noise density of the laser driver (assuming a white current noise). Noting that some commercial QCL drivers are specified with a current noise density of several nA/$\sqrt{}$Hz, our results show the importance of a proper choice of the QCL driver in applications requiring a narrow linewidth. This might be important for high-resolution molecular spectroscopy, but it becomes essential if one aims at significantly narrowing down the QCL linewidth using a servo-loop, e.g. by frequency stabilization to a high-finesse optical cavity using the Pound–Drever–Hall technique, which is our objective in the near future [20]. If the current noise of the driver increases, not only the overall laser frequency noise PSD rises, but also noise components of higher frequency contribute to the linewidth. As a consequence, the requirements on the feedback bandwidth needed to narrow the QCL linewidth, which is roughly given by the crossing point of the frequency noise spectrum with the β-separation line [30], become more stringent. The use of a low-noise laser driver as shown in this work enabled us to observe the inherent frequency noise of a free-running QCL without degradation from the current noise. This is an important advantage in view of the realization of an ultra-narrow linewidth QCL. The low-noise properties of our current source (350 pA/$\sqrt{}$Hz), combined with the low inherent frequency noise of our room-temperature QCL, indicate that a high reduction of the QCL linewidth can be obtained by frequency stabilization to an ultra-high-finesse optical cavity with a moderate feedback loop bandwidth on the order of 100 kHz. This is fully compatible with the QCL frequency modulation response. On the other hand, the use of a current source with a higher noise, as observed in some commercial QCL drivers, would push the required bandwidth to a value of some megahertz, which is much more challenging to achieve.

Acknowledgements The authors would like to thank Prof. Markus. W. Sigrist (ETH Zurich) for the loan of the absorption gas cell. This work was financed by the Swiss National Science Foundation (SNSF), by the Swiss Confederation Program Nano-Tera.ch which was scientifically evaluated by the SNSF, and by the Gebert-Ruef Foundation in Basel, Switzerland.

References

1. J. Faist, F. Capasso, D.L. Sivco, C. Sirtori, A.L. Hutchinson, A.Y. Cho, Science **264**, 553 (1994)

2. D.D. Nelson, B. McManus, S. Urbanski, S. Herndon, M.S. Zahniser, Spectrochim. Acta, Part A, Mol. Biomol. Spectrosc. **60**, 3325 (2004)
3. D.M. Sonnenfroh, W.T. Rawlins, M.G. Allen, C. Gmachl, F. Capasso, A.L. Hutchinson, D.L. Sivco, J.N. Baillargeon, A.Y. Cho, Appl. Opt. **40**, 812 (2001)
4. K. Namjou, S. Cai, E.A. Whittaker, J. Faist, C. Gmachl, F. Capasso, D.L. Sivco, A.Y. Cho, Opt. Lett. **23**, 219 (1998)
5. S. Borri, S. Bartalini, P. De Natale, M. Inguscio, C. Gmachl, F. Capasso, D.L. Sivco, A.Y. Cho, Appl. Phys. B, **85**, 223 (2006)
6. B.A. Paldus, T.G. Spence, R.N. Zare, J. Oomens, F.J.M. Harren, D.H. Parker, C. Gmachl, F. Capasso, D.L. Sivco, J.N. Baillargeon, A.L. Hutchinson, A.Y. Cho, Opt. Lett. **24**, 178 (1999)
7. R. Lewicki, G. Wysocki, A.A. Kosterev, F.K. Tittel, Opt. Express **15**, 7357 (2007)
8. B.A. Paldus, C.C. Harb, T.G. Spence, R.N. Zare, C. Gmachl, F. Capasso, D.L. Sivco, J.N. Baillargeon, A.L. Hutchinson, A.Y. Cho, Opt. Lett. **25**, 666 (2000)
9. J. Faist, C. Gmachl, F. Capasso, C. Sirtori, D.L. Silvco, J.N. Baillargeon, A.Y. Cho, Appl. Phys. Lett. **70**, 2670 (1997)
10. A.A. Kosterev, F.K. Tittel, C. Gmachl, F. Capasso, D.L. Sivco, J.N. Baillargeon, A.L. Hutchinson, A.Y. Cho, Appl. Opt. **39**, 6866 (2000)
11. D. Hofstetter, M. Beck, J. Faist, M. Nägele, M.W. Sigrist, Opt. Lett. **26**, 887 (2001)
12. M. Germer, M. Wolff, Appl. Opt. **48**, B80 (2009)
13. M. Beck, D. Hofstetter, T. Aellen, J. Faist, U. Oesterle, M. Illegems, E. Gini, H. Melchior, Science **295**, 301 (2002)
14. A. Castrillo, E. De Tommasi, L. Gianfrani, L. Sirigu, J. Faist, Opt. Lett. **31**, 3040 (2006)
15. C.H. Henry, IEEE J. Quantum Electron. **QE-18**, 259 (1982)
16. M. Yamanishi, T. Edamura, K. Fujita, N. Akikusa, IEEE J. Quantum Electron. **44**, 12 (2008)
17. T. Aellen, R. Maulini, R. Terazzi, N. Hoyler, M. Giovaninni, S. Blaser, L. Hvozdara, J. Faist, Appl. Phys. Lett. **89**, 091121 (2006)
18. A.L. Schawlow, C.H. Townes, Phys. Rev. **112**, 1940 (1958)
19. S. Bartalini, S. Borri, P. Cancio, A. Castrillo, I. Galli, G. Giusfredi, D. Mazzotti, L. Gianfrani, P. De Natale, Phys. Rev. Lett. **104**, 083904 (2010)
20. L. Tombez, J. Di Francesco, S. Schilt, G. Di Domenico, J. Faist, P. Thomann, D. Hofstetter, Opt. Lett. **36**, 3109 (2011)
21. T. Okoshi, K. Kikuchi, A. Nakayama, Electron. Lett. **16**, 630 (1980)
22. T.L. Myers, R.M. Williams, M.S. Taubman, C. Gmachl, F. Capasso, D.L. Sivco, J.N. Baillargeon, A.Y. Cho, Opt. Lett. **27**, 170 (2002)
23. G. Galzerano, A. Gambetta, E. Fasci, A. Castrillo, M. Marangoni, P. Laporta, L. Gianfrani, Appl. Phys. B **102**, 725 (2011)
24. J.-P. Tourrenc, Caractérisation et modélisation du bruit d'amplitude optique, du bruit de fréquence et de la largeur de raie de VCSELs monomode, Ph.D. dissertation, Université de Montpellier II, 2005
25. D.M. Baney, W.V. Sorin, in *Fiber Optic test and Measurements*, Chap. 5, ed. by D. Derickson (Prentice Hall, Englewood Cliffs, (1998)
26. D.S. Elliott, R. Roy, S.J. Smith, Phys. Rev. A **26**, 12 (1982)
27. P.B. Gallion, G. Debarge, IEEE J. Quantum Electron. **QE-20**, 343 (1984)
28. G.M. Stéphan, T.T. Tam, S. Blin, P. Besnard, M. Têtu, Phys. Rev. A **71**, 043809 (2005)
29. L.B. Mercer, J. Lightwave Technol. **9**, 485 (1991)
30. G. Di Domenico, S. Schilt, P. Thomann, Appl. Opt. **49**, 4801 (2010)
31. K.G. Libbrecht, J.L. Hall, Rev. Sci. Instrum. **64**, 2133 (1993)
32. R.W.P. Drever, J.L. Hall, F.V. Kowalski, J. Hough, G.M. Ford, A.J. Munley, H. Ward, Appl. Phys. B **31**, 97 (1983)
33. L.S. Rothman et al., J. Quant. Spectrosc. Radiat. Transf. **110**, 533 (2009)
34. E.E. Whiting, J. Quant. Spectrosc. Radiat. Transf. **8**, 1379 (1968)
35. D.K. Killinger, USF HITRAN-PC: Installation and software user manual (version 2.0), University of South Florida (1992)
36. J. Osinski, J. Buus, IEEE J. Quantum Electron. **QE-23**, 9 (1987)
37. A. Wittmann, Y. Bonetti, M. Fischer, J. Faist, S. Blaser, E. Gini, IEEE Photonics Technol. Lett. **21**, 814 (2009)
38. S. Bartalini, S. Borri, I. Galli, G. Giusfredi, D. Mazzotti, T. Edamura, N. Akikusa, M. Yamanishi, P. De Natale, Opt. Express **19**, 17996 (2011)